SciencePG
Science Publishing Group

Iron-doped BaTiO₃: Influence of iron on physical properties

Ashutosh Mishra, Niyati Mishra

School of Physics, Devi Ahilya University, Khandwa Road, Indore, India

Email address:

amishra1960@yahoo.co.in (A. Mishra), nmishra.sop@gmail.com (N. Mishra)

Abstract: Barium Titanate BaTiO3 is known for both its electric and magnetic properties. The synthesis and characterization of iron doped barium titanate; BaTi1-xFexO3 (x= 0.005, 0.01, 0.015) was investigated with a view to understand its structural, magnetic and electrical properties. A finest possible sample of Iron doped micro particles of BaTiO3 (BTO) with possible tetragonal structure via a solid-state route was prepared. Prepared samples of BaTi1-xFexO3 (Fe-BTO) were structural characterized by X-ray diffraction (XRD) then XRD data fitted by Rietveld refinement. Fourier Transform Infrared Spectroscopy were use to determine the Ti-O bond length position according to increment in Iron on Titanium site. The dielectric constant measurements of the samples were carried out at 1 MHz. Vibrating Sample Magnetometer (VSM) measurements revealed the magnetic nature of Iron doped BaTiO3. Magnetic Moment verses Temperature plot took at 1Tesla and Magnetic Moment verses Magnetic field plot took at low temperature (10K). Ferroelectric hysteresis loop traced at the electric field in-between -8 to +8 (KV/cm). Details of the preparation technique, experimental results, data analysis, and the interpretation will be presented.

Keywords: Iron Doped Barium Titanate, X-Ray Diffraction, Fourier Transform Infrared Spectroscopy, Dielectric Measurement, Magnetic Properties And Electrical Properties

1. Introduction

Barium titanate (BaTiO3) is one of the best known Perovskite ferroelectric compounds (A2+B4+O-3) that have been extensively studied [1, 2] due to the simplicity of its crystal structure, which can accommodate different types of dopant. This has led to the possibility of tailoring the properties [3] of doped BaTiO3 for specific technological applications, such as capacitors, sensors with positive temperature coefficients of resistivity, piezoelectric transducers and ferroelectric thin-film memories. Because of the intrinsic capability of the Perovskite structure to host ions of different size, a large number of different dopants can be accommodated in the lattice [4]. The mechanism of dopant incorporation into BaTiO3 has been extensively investigated and the behaviour of some transition metal ions has been well elucidated. The ionic radius is the main parameter that determines the substitution site [5].

Ferroelectric crystals, such as SrTiO3, BaTiO3, KNbO3, etc., represent an important class of perovskite material with the interesting prospects of technological applications ranging from electronic ceramic to constituents in optical devices. Most of the chemical activities and physical properties of these materials can be enhanced through the introduction of extrinsic and intrinsic dopants, such as transition metal cations doping, excess oxygen and oxygen vacancies. Understanding the effect of dopant on the electronic structure would be a key step to the elucidation of these properties.[6−13] Therefore, the nature of defects in ABO3 has been studied quite extensively both experimentally[5−10] and theoretically[14−17] in the last decades. Ternary oxide systems of the type ABO, with the perovskite structure are of interest due to their characteristic ferroelectric (i.e. KNbOr, BaTiO,) or incipient ferroelectric behaviour. Many applications and properties of these materials depend on their impurity content.

Barium titanate (BaTiO3) is another type of ABO3 perovskite, which has not only large ferroelectric response, but also very large nonlinear optical and electro-optic coefficients, which is attractive to designing nonlinear optical devices. These properties can be dramatically enhanced when they are doped with transition metals [8, 18−20].

Relaxer ferroelectrics are characterized by their broad

dielectric transition, known as the diffused phase transition with strong frequency dispersion. They have been the subjects of intense interests because they could be promising materials for use in non-volatile memory devices [21]. Up to now, the relaxor ferroelectric behaviour occurs mainly in the lead-based materials [22–24]. In order to develop environment-friendly materials, considerable studies have been focused on the lead-free materials [25–33]. It is well known that BaTiO3 has a paraelectric to ferroelectric transition at about 120 0C with a very high dielectric constant. Thus, considerable attentions were paid to the doped BaTiO3 [25–30] to modify the performance of the materials. However, the relaxer behaviour of the doped BaTiO3 was reported to occur at temperatures far above or below room temperature. Modified BaTiO3 is suitable for pyroelectric applications [34] as their infrared (IR) Response can be adjusted over a wide range of operating temperatures [35]. Our present focus is to develop Fe modified BaTiO3 materials to get a maximum IR response near room temperature, as room temperature IR sensors are attractive for a wide range of civilian and military applications [36, 37]. To achieve good sensing properties, it is necessary to produce fine and homogeneous powder. The structural and dielectric properties of the solid state route prepared Fe modified BaTiO3 are discussed in subsequent sections in order to establish their suitability as pyroelectric gas sensors.

The purpose of this paper is to throw some light on the influence of Fe impurity on the structure, Dielectric, Magnetic and Electrical properties of BaTiO3.

2. Experimental Details

Preparation of Fe doped BaTiO3: We started from highly pure fine powdered samples of BaCO3, TiO2 and Fe3O4 for bulk sample of doped BaTiO3. All these were mixed in the calculated molar ratio. Grinding the sample for 8-hours, and first heat treatment (calcinations) was given at 9000C for 12hour. After first calcinations, the material has again grinded for 4 hours at second heat treatment given at 11000C. After this, added the binder (poly vinyl alcohol gel) in powder sample and grind it for 4 hours once again. Make a pallet of the sample of about 15mm and take it again in furnace for sintering at 12500C for 12 hour.

2.1. Experimental Analysis by Different Methods

2.1.1. XRD

D8 Advance XRD: The XRD measurements were carried out using Bruker D8 Advance X-ray diffractometer. The x-rays were produced using a sealed tube and the wavelength of x-ray was 0.154 nm (Cu K-alpha). The x-rays were detected using a fast counting detector based on Silicon trip technology (Bruker Lynx Eye detector).

2.1.2. FTIR

The infrared absorption spectra were measured at room temperature, in the wave number range 4000 to 400 cm-1 by a computerized spectrometer type Jasco FTIR-300 (JAPAN)

using the KBr pellet technique. The samples were investigated as fine particles, which were mixed with KBr in the ratio (2:200mg powder to KBr respectively); the weighted mixture was then subjected to a pressure of 5t/cm2 to produce clear homogeneous discs.

2.1.3. Dielectric Constant Measurement

In Dielectric constant measurement, Dielectric-constant of Fe-BTO was recorded on hp- Hewlett Packard 4192 A, LF Impedance, 5 Hz – 13 Hz Analyzer. First a pallet of 15mm diameter of bulk sample was prepared and then coated both sides of the sample with low temperature silver paste. Put the sample in between two electrodes in furnace and obtain the value of Dielectric constant with variation of temperature manually.

2.1.4. Vibrating Sample Magnetization

The magnetization measurements on the Iron doped BTO samples were carried out using Quantum Design 14T PPMS-VSM.

2.1.5. Ferroelectric Loop

The loop between Polarization and Electric Field has been plotted on Ferroelectric hysteresis loop tracer Radiant Tech.

3. Results and Discussion

3.1. X-Ray Diffraction

X-ray diffraction (XRD) is a versatile, non-destructive technique that reveals the detailed information about the chemical composition and crystallographic structure of natural and manufactured materials. In Figure1 XRD patterns reports the single phase tetragonal crystal system of the space group P4mm (99) and pattern matched with the standard pattern JCPDS no. 79-2265. Diffraction data of Fe doped BaTiO3 has concluded that all major peaks of Fe-BTO are matching with reported XRD data of pure BTO and sample is in single phase. Which shows doping is perfect. The value of 2θ is in between 20 to 80º.
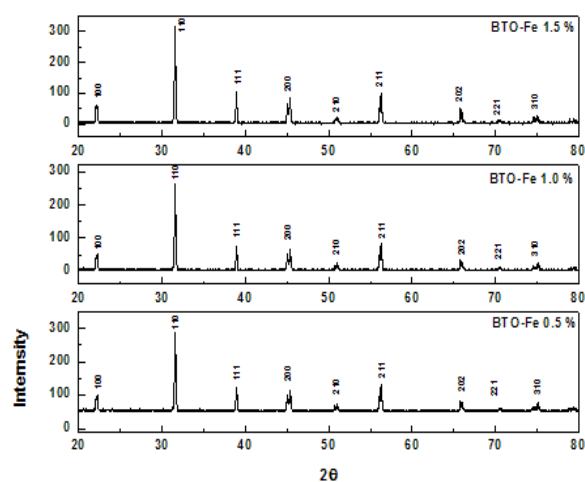
Figure 1. *X-ray Diffraction data of Fe doped BTO at different percentage doping.*

3.2. Fourier Transform Infrared Spectroscopy

Figure2 indicates FTIR spectra of Iron doped Barium Titanate (Fe-BTO) particles, synthesized at 1250 oC for 12 Hours. A broad absorption band in the range of 400-4000 cm-1 suggests the presence of considerable amount of H2O and OH in the particles [38, 39]. In particular the sharp absorption band at 3400 cm-1 was assigned to the stretching vibration of the Hydroxyl group with an intermolecular hydrogen bond, which shows the presence of hydroxyl group in palate made for FTIR by using KBr as a binder, used binder KBr is a sensitive material so moisture was expected. Also the sharp absorption band observed at around 532 cm-1 was attributed to the bending vibration of O6 octahedra deformation mode which was assigned by Slater [40] and confirmed by Spitzer [41].
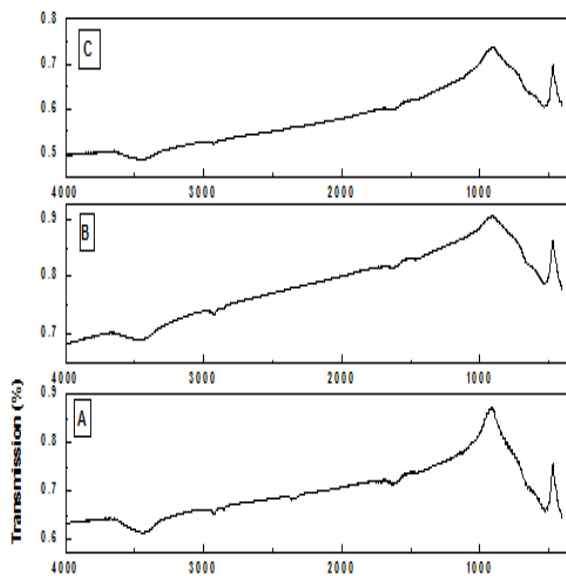
Figure 2. *FTIR data of Fe doped BTO at different percentage doping. [A] Fe= 0.5 %, [B] Fe= 1.0 % and [C] Fe= 1.5%.*

Strong absorption peak appears near 500 cm-1. This peak characterizes the vibration of Ti-O bond. When the concentration of Fe increases, another effect exhibits. The wavenumber of the absorption peak increases with increase of the concentration of Fe. It's been observed that the absorption wavenumber of Ti–O bond become shifted to higher side with increase of the concentration of Fe. The value of the wavenumber increases from around 500 cm-1 to 523 cm–1 when the concentration of Fe changes from 0.00 to 0.005, 540 cm–1 when Fe=0.01 and 547 cm–1 when Fe= 0.015. It indicates the decrease of the cell size. The length of Ti-O bond is shortened by replacement of Fe. Then the interaction between Ti and O bond is enhanced. Cell size decreases accordingly.

3.3. Dielectric Measurements

Barium titanate is a cubic paraelectric above 1200C. Below this temperature, it is ferroelectric, with a tetragonal structure down to 50C. Considerable effort has been devoted to understanding the behaviour of the dielectric constants of Fe-BTO. In Dielectric-constant measurement, the transition temperature of Fe-BTO is occurring at 1250C. The reported value of transition temperature (Curie- temperature) of pure BTO is 1200C.

In Figure 3 one can see that after doping Fe in pure BTO, on increasing the temperature on higher side, the transition temperature was shifted from 1200C to 1250C. While on cooling the sample, the transition temperature was shifted to 1100C. Dielectric constant measurements of the sample above and below the Curie temperature were carried out at 100 Hz, the Transition temperature is found shifted towards higher side from that of pure BaTiO3. The Thermal Hysteresis is indicative of the fact that the transition is indeed of First Order.

Figure 3 shows the temperature dependence of dielectric constant for different Fe ion concentration substituted at the Ti site of BTO. The Curie temperature is defined as the temperature corresponding to the maximum dielectric constant. The dielectric constant at room temperature (PRT) increased gradually with an increase in temperature up to its maximum value (PMax) at Tc and then decreased [42-49]. The values of dielectric constant for Fe modified BaTiO3 were lower compared to pure BaTiO3 due to the addition of Fe ion as reported by other researchers [45, 46, and 50]. The dielectric studies indicated a shift in the transition temperature (Tc) towards the lower temperature side with an increase in Fe content. The value of (Tc) decreased due to the addition of Fe^{+3} ion in the Ti^{+4} sites, as the lower valence state of Fe^{+3} ion created an oxygen vacancy leading to a break in the cooperative vibration of the Ti–O chains [49]. Let us call TM as the temperature at which the maximum of Dielectric constant (ε) occurs. It corresponds to the passage of the quadratic to cubic symmetry phase. For the Fe-doped crystals, TM decreases according to concentration as shown on Fig. 4. We observe in Fig. 3 that on increasing the Fe concentration in the crystal, the value of ε at maximum increases whereas the ε(T) curve appears to exhibit a broader peak.
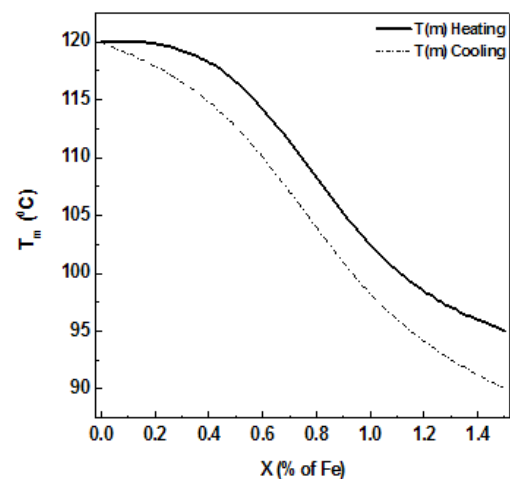

Figure 4. *Variation of T_m against Fe concentration.*
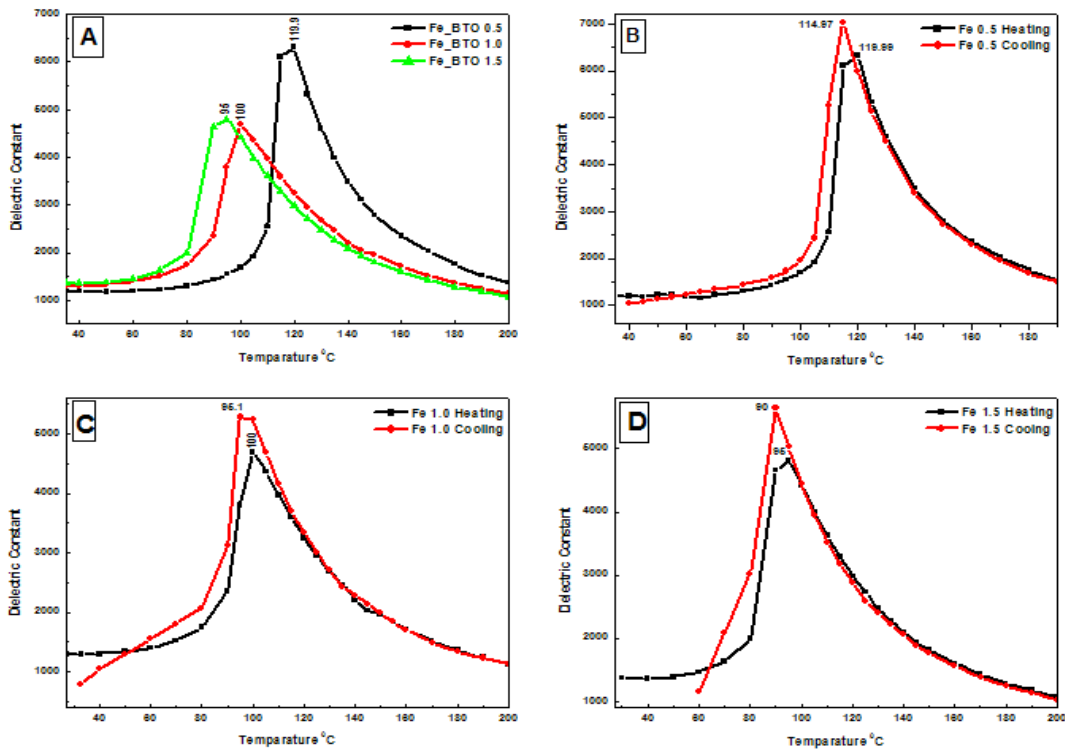
Figure 3. *Dielectric constant Vs. Temperature data of Fe doped BTO at different percentage doping. [A] Shows the fall of Tc at different Fe concentration [B] shows the hysteresis at Fe=0.5 % by heating and cooling simultaneously [C] shows the hysteresis at Fe=1.0 % by heating and cooling simultaneously and [D] shows the hysteresis at Fe=1.5 % by heating and cooling simultaneously.*

3.4. Magnetic Measurement

Magnetic measurements of the Fe doped BTO samples have been done on Vibrating Sample magnetometer. In Figure5 it shows a good deal with magnetic moment of increasing Fe % on BTO.
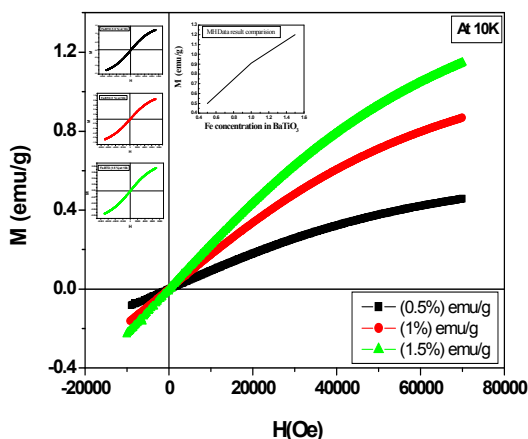
Figure 5. *Magnetic measurement plot of VSM. The most left insert shows the full hysteresis view. The centre insert shows the increment of magnetic moment with respect to increasing percentage doping on Iron on Ti site at BaTiO3.*

In Figure6 one can see the interaction in between paramagnetic and ferromagnetic behavior.

Note that even for the all samples with low oxygen vacancy concentration, not all Fe dopant ions are ferromagnetically coupled. The measured magnetic moment is attributed to isolated paramagnetic and ferromagnetically coupled Fe dopant ions which can be observed in Figure 6.

The paramagnetic component dramatically decreases with increasing Fe % in BTO. Even though ferromagnetism has been obtained in all Fe-BTO, the small magnetic moment value as compared with other typical ferromagnetic materials should be noticed, and its ferroelectricity deteriorated by the large leakage current caused by the oxygen vacancies. Ederer and Spaldin [39] have explained the difficulty realizing multiferroic perovskites [40, 41] and they clarified the exclusivity between ferromagnetic and ferroelectric order in the BaTiO3 system. To stabilize the off-centring of Ti ions which is essential for ferroelectricity, an energy-lowering covalent bond has to be formed, which requires empty d orbitals of the transition metal ions. However, the substitution of Ti ions by Fe ions destroys the stabilization of the off-centring displacement, which weakens the polarization as shown in the PE loops (as reported in

Figure7).On the other hand, a partially occupied d shell of transition metal ions is needed for magnetization. Moreover, the ferromagnetic coupling[42] between Fe ions happens

when a low concentration of oxygen vacancies is present, which increases the leakage current and thus further deteriorates PE.
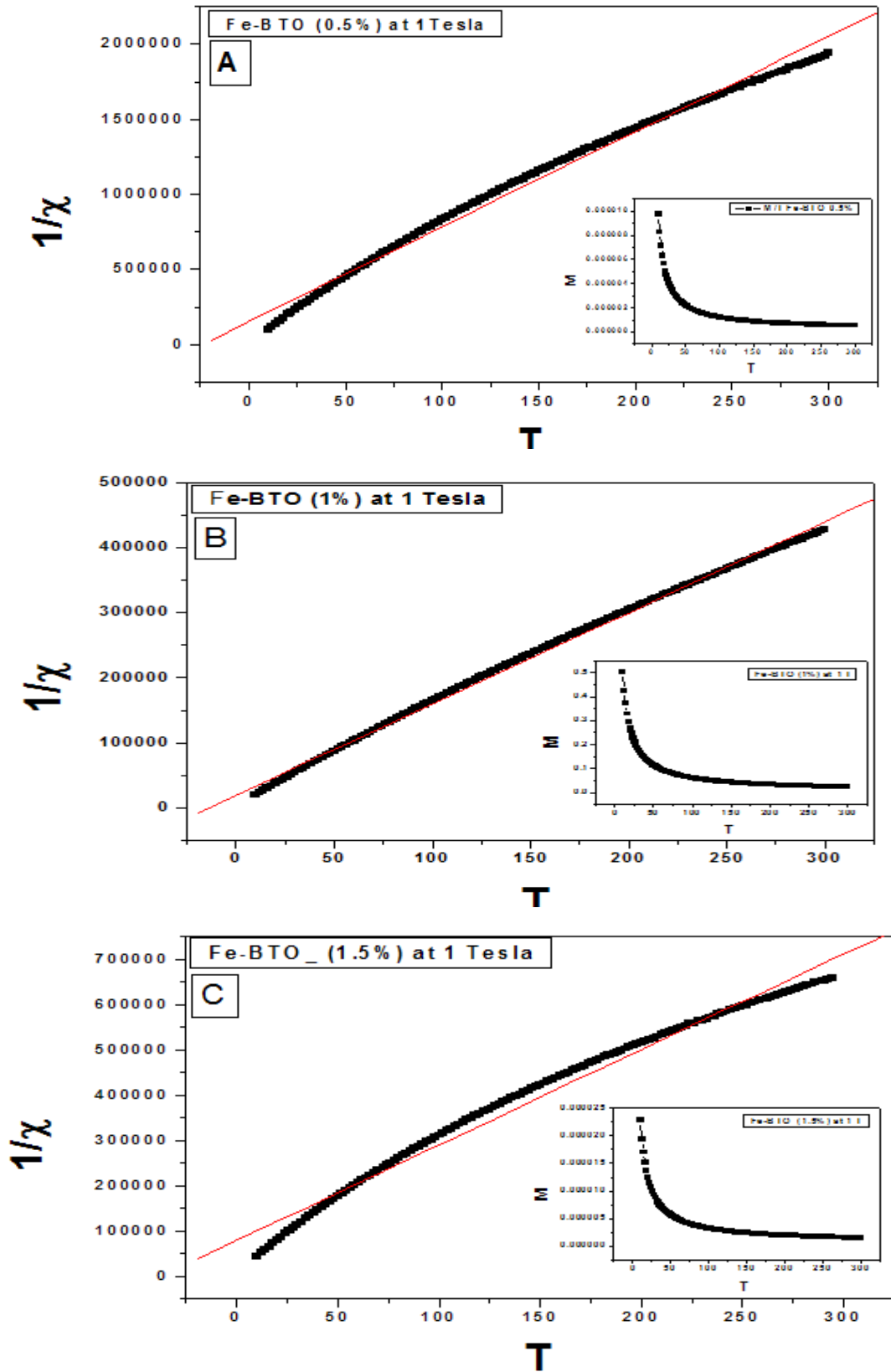

Figure 6. *1/χ plot of Fe doped BTO at different percentage doping.[A] Fe= 0.5 %, [B] Fe= 1.0 % and [C] Fe= 1.5%. Insert shows the M over T Plot.*
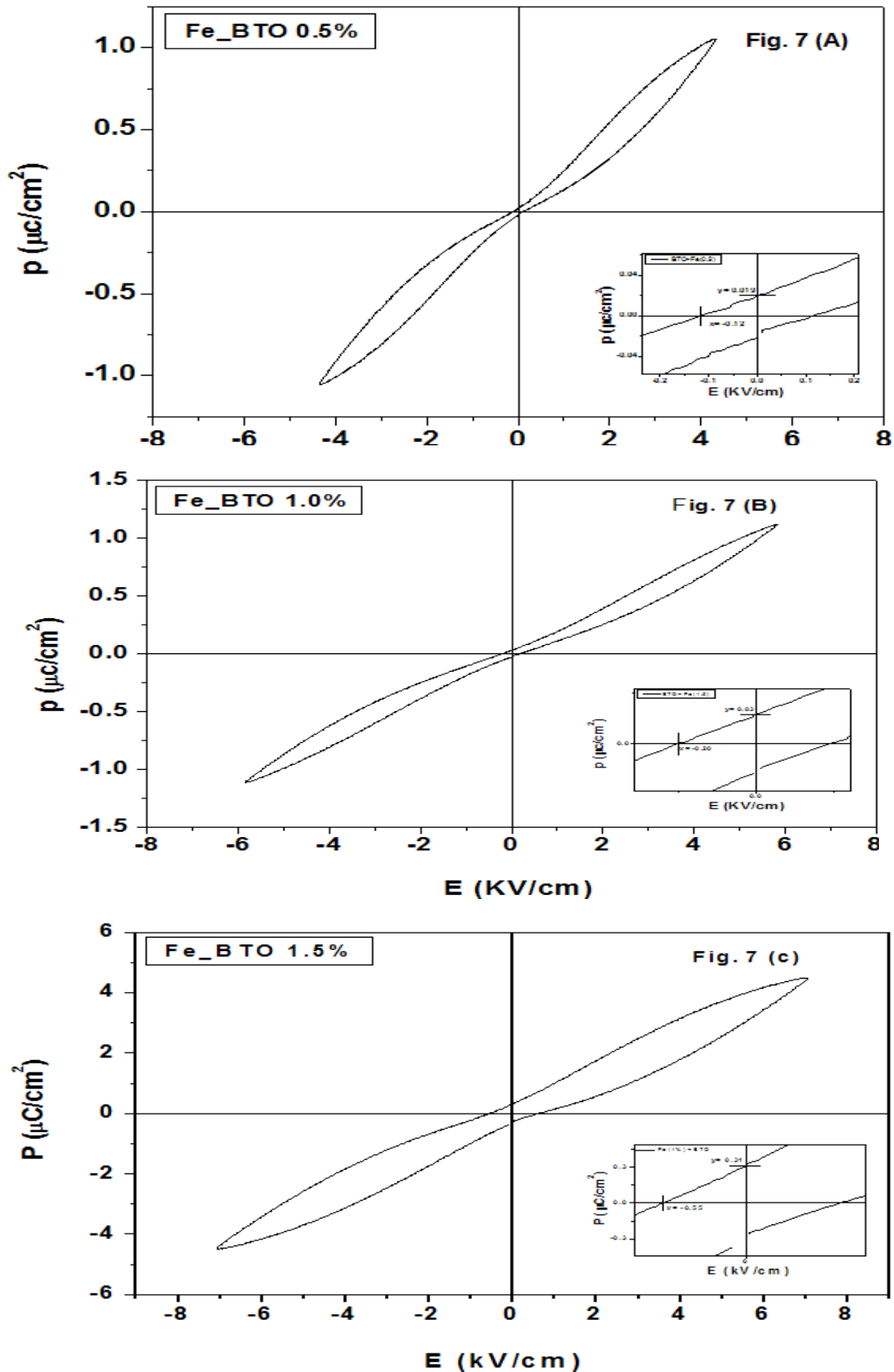
Figure 7. *Ferroelectric hysteresis plot of Fe doped BTO at different percentage doping. [A] Fe= 0.5 %, [B] Fe= 1.0 % and [C] Fe= 1.5%.*

3.5. Electrical Measurement

The loop between Polarization and Electric Field has been plotted on Ferroelectric hysteresis loop tracer Radiant Tech of all Fe doped BTO samples. The P–E loops indicate a typical ferroelectric (FE) behavior. The remnant polarization Pr and coercive electric field Ec of all samples shown in Table1. The P-E loop has been traced for applied voltages

and they are exhibited in Figure7 for x=0.005, 0.01 and 0.015, respectively.

Further attempts to reach saturation or to track for breakdown field have not been investigated. In the present study, we have only focused on investigating for existence of the ferroelectric loop. The loss decreases with an increase in the level of doping. The defect reaction proposed in the BaTiO3 systems is the formation of vacancies at B site. As we have (Ti4+) excess in our starting compositions, the possibility of the formation of Ti vacancies can be ruled out. There are different views regarding the defect mechanism for doped and pure barium titanate.

Table 1. Comparative data of all samples from Figure 4.

Fe doped BaTiO$_3$	Remnant Polarization P$_r$ (μC/cm^2)	Coercive Field E$_c$ (KV/cm)
BaTi$_{0.995}$Fe$_{0.005}$O$_3$	0.018	-0.12
BaTi$_{0.99}$Fe$_{0.01}$O$_3$	0.030	-0.20
BaTi$_{0.985}$Fe$_{0.015}$O$_3$	0.310	-0.66

4. Conclusion

The compositions synthesized by solid state route are single phase. XRD patterns reports the single phase tetragonal crystal system of the space group P4mm (99) and pattern matched with the standard pattern JCPDS no. 79-2265. The additive Fe doped into BaTiO3 ceramics. The FTIR spectra reveal that they affect the vibration of crystal lattices. So, the ordinary structure of TiO6 octahedron is distorted or damaged. The wavenumber of absorption peak decreases. A study about the correlation between phase transition, spontaneous polarization and FTIR in doped BaTiO3 system is in progress. Experimentally, the Curie temperature Tc can be determined by measuring the dielectric permittivity ε versus temperature: Tc is identified with the temperature TM of the maximum of Ip and to the temperature TM of the maximum of the dielectric permittivity ε. The cubic-quadratic transition of BaTiO3 is influenced by Fe and other dopings; TM decreases and transition becomes more diffuse for high rates of doping agents. Transition could disappear for very large quantities of inserted ions, such as Fe. The measured variations of ε-1(T) are in agreement with the thermodynamic approach of Devonshire [55] for a first-order transition, with the Curie constants doubling when the system passes from the ferroelectric phase to the paraelectric phase in BaTiO3. The electric properties depend strongly on the oxygen vacancy concentration which is controlled by the deposition pressure and are also significantly influenced by doping with Fe. The leakage current is decreased by the substitution of Ti by Fe ions which form trapping centres in the BaTiO3 band gap. The dielectric constant decreases and dielectric loss increases as compared with the pure BaTiO3 sample. The Fe-doped BaTiO3 samples with a large amount of oxygen vacancies show room-temperature ferromagnetic behavior. On the contrary, neither the Fe- doped BaTiO3 samples with low oxygen vacancy concentration nor the pure BaTiO3

with high oxygen vacancy concentration exhibit ferromagnetism. The present work shows the dependence of the electric and magnetic properties on the Fe-doping and oxygen vacancy of the BaTiO3 samples; although doping with Fe can decrease the leakage current, which is very important for device application, the ferroelectricity is impaired. Besides, sole Fe doping is not enough for introducing room-temperature ferromagnetism, since oxygen vacancies are also necessary, but unfortunately they increase the leakage current. Therefore, the ferroelectricity and ferromagnetism can be tuned mutually by doped-Fe and undoped BaTiO3, so that they are also coupling each other mutually in Fe-doped BaTiO3.

References

[1] D. Makovec, Z. Samadmija and M. Drofenik, J. Am. Ceram. Soc. 87, 1324 (2004).

[2] D. Maga, P. Igor and M. Sergei, J. Mater. Chem. 10, 941 (2000).

[3] A. Jana, T. K. Kundu, S. K. pradhan and D. Chakravorty, J. Appl. Phys. 97 (4), 44311 (2005).

[4] Z. Jin, C. Ang and Z. Yu, J. Am. Ceram. Soc. 82(5) 1345 (1999).

[5] P. Yongping, Y. Wenhu and C. Shoutian, J. Rare Earths. 25, 154 (2005).

[6] P. Gunter and J.P. Huignard, (ed) Photorefactive Materials and their Application I and II (Berlin: Springer), (1998).

[7] R. Waser, T. Bieger and J. Maier, Solid State Commun.76, 1077, (1990).

[8] W.T. Wang, G. Yang, P. Duan, Y. L. Zhou and Z. H. Chen, Chin. Phys. Lett. 19 1122, (2002).

[9] C. Ang, Z. Yu, Z. Jing, P. Lunkenheimer and A. Loidl, Phys. Rev. B 61 3922 (2000).

[10] T. Higuchi, T. Tsukamoto, K. Kobayashi, I. Ishiwata, M. Fujisawa, T. Yokoya, S. Yamaguchi and S. Shin, Phys. Rev. B 61 12860 (2000).

[11] Q. B. Liu, R. Q.Li, Y. Z.Zeng and Z.Z. Zhu, Acta Phys. Sin. 55 0873 (in Chinese) (2006).

[12] M. Z. Yao, M. Gu and F. S. Liu, Chin. Phys. 12 0084 (2003).

[13] F. S. Liu, M. Gu and R. Zhang, Chin. Phys. 13 1931 (2004).

[14] M. O. Selme, P. Pecheur and G. Toussaint, J. Phys. C 17 5185

(1984).

[15] F. M. Michel-Calendini and K. A. Muller, Solid StateCommun. 40 255 (1981).

[16] R. A. Evarestov, S. Piskunov, E. A. Kotomin and G. Borstel,Phys. Rev. B 67 064101 (2003).

[17] R. Astala and P. D. Bristowe, Modelling Simul. Mater.Sci. Eng. 9 415 (2001).

[18] W. S. Shi, Z. H. Chen, N. N. Liu, H. B. Liu, Y. L. Zhou, D.F. Cui and Z. H. Chen, Appl. Phys. Lett., 75, 1547, (1999).

[19] G. Yang, H. H. Wang, G. T. Tan, A. Q. Jiang, Y. L. Zhou, G. Z. Yang and Z. H. Chen, Chin. Phys. Lett., 18, 1598, (2001).

[20] W. F. Zhang, Y. B. Huang, M. S. Zhang and Z. G. Liu, Appl. Phys. Lett. 76, 1003, (2000).

[21] B.H. Park, B.S. Kang, S.D. Bu, T.W. Noh, J. Lee, W. Jo, Nature 401, 682–684 (1999).

[22] L.E. Cross, Ferroelectrics 151,305 (1994).

[23] N. Setter, L.E. Cross, J. Appl. Phys. 51, 4356 (1980).

[24] H. Ardnt, F. Sauerbier, G. Schmidt, A. Shebanov, Ferroelectrics 79, 145 (1988).

[25] G.A. Smolenski, V.A. Isupov, Dokl. Akad. Nauk. SSSR 9, 653 (1954).

[26] G.A. Smolenskii, V.A. Isupov, A.I. Agranovskaya, S.N. Popov, Sov. Phys. Solid State 2, 2584 (1961).

[27] R.M. Glaister, J. Am. Ceram. Soc. 43, 348 (1960).

[28] P. Gallagher, J. Am. Ceram. Soc. 46, 359 (1963).

[29] A.I. Kashilinski, V.I. Chechernikov, Yu.N. Venevtsev, Sov. Phys. Solid State 8, 2074 (1967).

[30] I.H. Ismailzade, R.M. Ismailov, Phys. Stat. Sol. (a) 59, K191 (1980).

[31] M. Mahesh Kumar, M.B. Suresh, S.V. Suryanarayana, G.S. Kumar, J. Appl. Phys. 6811, 84, (1998).

[32] M. Mahesh Kumar, M.B. Suresh, S.V. Suryanarayana, J. Appl. Phys. 86, 1634 (1999).

[33] Chen Ang, Zhi Yu, Zhi Jing, Phys. Rev. B 61, 957 (2000).

[34] J. M. Herbert, Ferroelectric Transducer and Sensors, Gordon and Breach, New York (1980).

[35] M. S. Mohammed, G. W. Auner, R. Naik, J. V. Mantese, N. W. Schubring, and A. L. Micheli, J. Appl. Phys. 84, 3322 (1998).

[36] D. A. Scribner, M. K. Kruer, and J. M. Killiany, Proc. IEEE 79, 66 (1991).

[37] E. L. Dereniak and D. G. Crowe, Optical Radiation Detectors, Wiley, New York, (1984).

[38] R. Vivekanandan, S. Philip and T. N. Kutty, Mater.Res.Bull., 22, 99 (1986).

[39] D. Hennings and S. Schreinemacher, J.Eur.Ceram.Soc., 9, 41 (1992).

[40] J. C. Slater, Phys.Rev., 78, 448 (1950).

[41] W. G. Spitzer, R. C. Miller, D. A. Kleiman and L. E. Howarth, Phys.Rev., 126, 1710 (1962).

[42] K. S. Mazdiyasni, R. T. Dolloff, and J. S. Smith, J. Am. Ceram. Soc., 52, 523 (1969).

[43] M. P. Pechini, US Patent no. 3, 330, 697 (11 July 1967).

[44] M. Kakihana, M. Arima, M. Yashima, M. Yoshimura, Y. Nakamura, H. Mazaki, and H. Yasuoka, Sol-Gel Science and Technology (The American Ceramic Society, Columbus, OH,), p. 65, (1994).

[45] R. Vivekanandan and T. R. N. Kutty, Ceram. Int. 14, 207 (1988).

[46] K. Fukai, K. Hidaka, M. Aoki, and K. Abe, Ceram. Int. 16, 285 (1990).

[47] M. Leoni, M. Viviani, P. Nanni, and V. Buscaglia, J. Mater. Sci. Lett. 15, 1302 (1996).

[48] J. W. Liou and B. S. Chiou, J. Am. Ceram. Soc. 80, 3093 (1997).

[49] J. T. Last, Phys. Rev. 105, 1740 (1957).

[50] G. Arlt, D. Henningsand, and G. deWith J. Appl. Phys. 58, 1619 (1985).

[51] C. Ederer and N. A. Spaldin, Nat. Mater., 3, 849, (2004).

[52] J. J. Li, J. Yu, J. Li, M. Wang, Y. B. Li, Y. Y. Wu, J. X. Gao and Y. B. Wang, Acta Phys. Sin., 59, 1302, (2010).

[53] D. Y.Guo, C. Li, C. B. Wang, Q. Shen, L. M. Zhang, R. Tu and T. Goto, Acta Phys. Sin., 59, 5772, (2010).

[54] Q. X. Zhao, J. K. Ma, B. Geng, D. Y. Wei, L. Guan and B. T.Liu, Acta Phys. Sin. ,59, 8042, (2010).

[55] A. F. Devonshire, Phil. Mag., 40, 1040 (1949).